SPE 56599

Perforation Design for Fracture Stimulated Wells, A Finite Element Method

A. Ebrahim, SPE, Kuwait University, C. Mark Pearson,* SPE, and D. V. Griffiths, Colorado School of Mines.

* also with CARBO Ceramics, Inc.

This paper was prepared for presentation at the 1999 SPE Annual Technical Conference and Exhibition held in Houston, Texas, 3–6 October 1999.

Abstract

The effects of perforation orientation and phasing on hydraulic fracture initiation have been investigated as a function of the in-situ stress field and stress-anisotropy using a three-dimensional finite element model. The results of the finite element analyses are used to determine the mode of fracture initiation in the perforation tunnel. If the perforation is oriented away from the preferred fracture plane, multiple fractures, S-shaped fractures, and T-shaped fractures are shown to initiate. If a perforation is oriented toward the preferred fracture plane, a single vertical fracture is initiated.

A correlation between stress-anisotropy and the critical perforation orientation angle, which insures the initiation of a single vertical fracture, was developed. The maximum allowable deviation angle from the preferred fracture plane, that insures the initiation of a single vertical fracture for a given stress-anisotropy value, is presented. This information, as a function of stress anisotropy, can be directly applied to field operations in which a perforation schedule is desired in order to facilitate creation of a single bi-wing planar fracture.

Introduction

Perforation orientation and phasing play an important role in the success of hydraulic fracturing operations. Away from the wellbore, fractures propagate in the direction perpendicular to the direction of the minimum principal stress (preferred fracture plane).[1,2] Thus, it is desirable for the fracture to initiate in the same plane.

Fracture initiation is strongly dependent on the in-situ stress field. Therefore, perforation orientation and phasing become crucial aspects of the hydraulic fracturing operation. If the perforations are not properly designed, many fractures may initiate in different places on the wellbore wall and perforation tunnels.[1,2] As a result, different fracture geometries may be induced near the wellbore region. These different fracture geometries may cause serious problems such as premature screenout, proppant bridging, narrow fracture width, and a tortuous path can result from a poor perforation design. Some researchers believe that the above problems can be solved by other techniques, such as proppant slugs and control of fluid viscosity. However, why should these problems be solved when they can initially be eliminated by a proper perforation orientation and phasing design?

Haimson and Fairhurst[1] conducted a series of experiments to investigate the effect of an in-situ stress field around the wellbore on fracture initiation for porous permeable materials. They concluded that vertical fractures propagate in the direction perpendicular to the minimum horizontal stress. Behrmann[2] performed some experiments where he tried to simulate real downhole conditions. Behrmann found, for a single stress-anisotropy value, that the perforation must be oriented within a small angle with respect to the plane perpendicular to the minimum horizontal stress for the fracture initiation to occur at the perforation.

Morales et al[3] investigated fracture initiation from a deviated wellbore by using a three-dimensional fracture model. They concluded that two or more axial or transverse fractures might be induced. These fractures interact and eventually reorient themselves toward the preferred fracture plane. Weng[4] used a two-dimensional boundary element fracture model to further investigate the interaction between the induced fractures. Moreover, he investigated the link-up of the starter fractures initiated from perforations of deviated wellbores, and provided conditions under which the starter fractures link-up. Yang et al[5] used a technique based on a two dimensional finite element solution to the stress distribution of a pressurized vertical wellbore with pre-existing fractures to simulate the fracture initiation problem. They claimed that starter fractures can be initiated either from the preferred direction on the wellbore wall or from the tip of a pre-existing

fracture which may be oriented in a plane other than the preferred fracture plane. The position of fracture initiation is a function of the angle of the pre-existing fracture to the preferred fracture plane and the ratio of the two principal horizontal stresses. The initiation of starter fractures at orientations other than the preferred plane implies fracture reorientation; therefore, near-wellbore tortuosity. Akgun et al[6] used a two-dimensional finite element package (ANSYS) and a three-dimensional boundary element fracture analysis code (FRANC3D). Both models assume linear elastic mechanics to investigate fracture initiation from vertical wellbores under high in-situ stress conditions. The objective of the study was to determine the location, the geometry, and the breakdown pressure of fractures initiating from non-circular wellbores in the presence of various pre-existing (natural or shear-induced) fractures or perforations. The following are the conclusions of their study:

- While non-circular borehole geometries resulting from borehole breakout slightly reduce wellbore breakdown pressure, they do not play any significant role in the initiation of hydraulic fractures.
- In an uncased vertical wellbore, induced shear fractures, which lead to borehole breakouts, may provide sites for multiple fracture initiation. The non-ideal locations (with respect to the location of the least compressive stress around the borehole wall) of these induced shear fractures would require any initiated hydraulic fractures to reorient towards the preferred fracture plane. As a result, near-wellbore tortuosity and narrow fracture width are created. This will ultimately increase the chance of screenout.

The objective of this study; however, is to investigate the effects of perforation orientation and phasing on hydraulic fracture initiation as a function of the in-situ stress field and stress-anisotropy, using a three-dimensional finite element model. Also, casing, cement, and formation material properties were considered in this study.

Finite Element Modeling

In finite element analysis, the body to be modeled is subdivided into small finite elements. The subdivided body is called the mesh. Since the objective of this study is to investigate the effects of perforation orientation and phasing on fracture initiation, two different three-dimensional meshes were developed to model the effects of perforation orientation and phasing on fracture initiation. The first mesh is generated to model a single perforation as shown in Figure 1. This mesh is used to determine the shapes of the induced fractures (single vertical fracture, multiple parallel fractures or S-shaped fractures, and axial or T-shaped fractures). Also, a correlation between stress anisotropy and the critical perforation orientation angle was developed using the single perforation mesh. The correlation determines whether or not a single vertical fracture initiates for a desired perforation angle as a function of stress anisotropy. The second mesh is generated to model a full wellbore with two perforations as shown in Figure 2. This mesh is used to investigate the effects of perforation phasing on fracture initiation. The two meshes are highly unstructured meshes that can be refined in the axial direction, radial direction, and tangential direction.[7]

A general finite element program for three-dimensional elastic analysis was developed from the system of programs published by Smith and Griffiths (ref. 8). The finite element program is used to determine the locations of fracture initiation. The general procedure is as follows:

- Read the input data file.
- Apply the in-situ stress field.
- Calculate nodal displacements and strains.
- Calculate the stresses at the Gauss points (integration points) within the elements using the above-calculated strains.
- Use Mohr-Coulomb failure criterion or tensile failure criterion to ascertain whether or not failure occurred at the Gauss points within the elements.

Applying the In-Situ Stress Field

Drilling a circular hole alters the original stress field at some depth. The new stress field around the wellbore is referred to as the in-situ stress field. The in-situ stress field around the wellbore is the most important parameter that influences the fracture initiation and propagation. The vertical stress (σ_v) is constant for a constant depth. The following equations are used to model the alteration in the stress field around the wellbore: [9-12]

$$\sigma_r = \frac{(\sigma_{H\min} + \sigma_{H\max})}{2}\times\left(1-\frac{r_w^2}{r^2}\right)+\frac{(\sigma_{H\min} - \sigma_{H\max})}{2} \times\left(1-\frac{4r_w^2}{r^2}+\frac{3r_w^4}{r^4}\right)\times\cos(2\theta)+\frac{r_w^2}{r^2}\Delta P \quad (1)$$

$$\sigma_\theta = \frac{(\sigma_{H\min} + \sigma_{H\max})}{2}\times\left(1+\frac{r_w^2}{r^2}\right)-\frac{(\sigma_{H\min} - \sigma_{H\max})}{2} \times\left(1+\frac{3r_w^4}{r^4}\right)\times\cos(2\theta)-\frac{r_w^2}{r^2}\Delta P \quad (2)$$

$$\tau_{r\theta} = \frac{(\sigma_{H\min} - \sigma_{H\max})}{-2}\times\left(1+\frac{2r_w^2}{r^2}-\frac{3r_w^4}{r^4}\right)\times\sin(2\theta) \quad (3)$$

Mohr-Coulomb and Tensile failiure criterion were used in the simulation runs to determine whether or not a fracture is initiated. Fracture initiated on the same locations when tensile failure criteria and Mohr-Coulomb failure criteria were used.

For a tensile failure criteria, a failure occurs when the least principal stress, σ_3, exceeds the tensile strength of the rock. In this case, the Gauss point fails and a fracture initiates when:

$$\sigma_3 \geq \sigma_T \quad (4)$$

Effects of Perforation Orientation on Fracture Types

Different perforation orientations were simulated to ascertain the position of the hydraulic fracture initiation along the perforation tunnel and thus, identifying the different fracture types. Figures 3 and 4 show the approach taken to identify different fracture types. To identify the fracture type, a horizontal plane is cut at the top of the perforation and another horizontal plane is cut at the center of the perforation. Different fracture types are identified based on the fracture initiation positions along the perforation tunnel. Figure 3-A illustrates a horizontal plane cut at the top of the perforation. The shape of the fractures in Figure 3-A suggests a single vertical fracture since the fracture initiated at the top or the bottom of the perforation in the vertical plane. Another way to identify a single vertical fracture is to cut another horizontal plane at the center of the perforation, and no fractures should be detected at the sides of the perforation as shown in Figure 3-B. Figure 4-A illustrates a horizontal plane cut at the center of the perforation. Multiple fractures are identified when the fractures on both sides of the perforation do not initiate from the same position along the perforation tunnel. If the fractures on both sides of the perforation initiate from the same distance along the perforation tunnel and the fractures have the same length, the fracture induced is identified as an axial fracture as shown in Figure 4-B.

Perforation angles from 0° to 90° relative to the direction of minimum horizontal stress were investigated in 5° and 10° increments to model the effects of perforation orientation on fracture initiation behavior (different fracture types). Perforation length, diameter, and the material properties of casing, cement, and sandstone were constants, as shown in Table 1.

Results and Discussions

Different fracture types were induced as a result of changing the perforation orientation. A single vertical fracture, multiple-parallel fractures, S-shaped fractures, and axial fractures were induced when the perforation orientation was changed. Results of the simulation runs are summarized in Table 2. Fracture discontinuity appears in the visualization figures (e.g. Figure 4) because in these runs the mesh used was not refined in the axial direction, along the perforation tunnel. Instead, the mesh was refined in the theta direction to investigate the different fracture types induced. In subsequent runs the mesh was refined in the axial direction, and coarse in the theta direction, to verify that the fracture was continuous along the perforation wall. . An example result is shown in Figure 5 where the fracture is continuous in nature due to the refined mesh in the axial direction.

Because of the limitations in computer resources, the mesh should be refined only in the desired direction based on the objective of the study. Thus, the axial fracture discontinuity shown in the visualization figures where the mesh is refined in the theta direction should be disregarded.

Vertical Fractures

A single vertical fracture is initiated from the top and bottom of the perforation when the perforation was aligned to the preferred plane, perpendicular to the direction of the minimum horizontal in-situ stress (90°). This is illustrated in Figure 6 by the dark line in the center of the perforation. Figure 6 shows a horizontal cut of a plane at the bottom of the perforation, notice that only a single fracture is initiated along the entire perforation length.

A horizontal plane is cut at the center of the perforation to check whether or not a fracture is initiated at the sides of the perforation. It is observed that a fracture did not initiate at the sides of the perforation as illustrated in Figure 7.

Nonplanar Fracture Geometry

Fractures that do not initiate in the vertical plane only are described as nonplanar fractures.[13,14] Nonplanar fractures may be categorized as multiple-parallel fractures, S-shaped fractures, axial fractures, and T-shaped fractures. The above fractures are dependent on the perforation orientation angle with respect to the in-situ stress field.

Multiple-Parallel Fractures and S-Shaped Fractures

Multiple-parallel fractures and S-shaped fractures initiated in this study when the perforation orientation was greater than 5° and less than 85° for a 4,000-psi stress anisotropy. Different perforation orientations, as listed in Table 2, were simulated to ascertain the fracture initiation position. Figures 8 and 9 illustrate horizontal cuts at the center of the perforations that are oriented at 60° and 30° respectively. Multiple fractures initiate at different locations along the sides of the perforation tunnel. Fracture initiation behavior suggests that multiple-parallel and S-shaped fractures are initiating along the perforation tunnel.

Axial Fractures

Axial fractures may be induced when the perforation orientation is parallel or slightly deviated from the direction of the minimum horizontal in-situ stress. Axial fractures are defined as the fractures that can potentially initiate at the vertical plane of the perforation (along the perforation) and at the sides of the perforation. Horizontal planes are cut at the center and the bottom of the perforations that are oriented at 5° and 0° to ascertain the fracture initiation position. Figures 10

and 11 show that fractures initiate at the vertical and horizontal plane of the perforation that is oriented at 0°. Figure 12 illustrates a vertical plane cut through the perforation. It is obvious that fractures initiated at every position around the perforation.

Critical Perforation Orientation Angle

What is the value of stress anisotropy that affects fracture initiation? How does stress anisotropy affect the induced fracture type? What is the maximum allowable deviation angle from the preferred fracture plane that insures the initiation of a single vertical fracture? Is the maximum deviation angle from the preferred fracture plane the same for different stress anisotropy values? If not, what is the critical perforation orientation angle to create a single vertical fracture for a given stress anisotropy?

Many researchers in the petroleum industry have frequently asked the above questions. The answers will help petroleum engineers to efficiently design the hydraulic fracturing operation. A classical bi-wing fracture, for vertical wells, is desired in the hydraulic fracturing operation because it provides an excellent flow path for the proppant to be successfully placed in the induced fractures. Initiation of a classical bi-wing fracture is a function of two parameters:

1. Perforation orientation.
2. Stress anisotropy.

The critical perforation orientation angle within which a single vertical fracture initiates, is strongly dependent on the stress anisotropy. For instance, if the stress anisotropy is 0 psi, a single vertical fracture initiates from perforations that are oriented at any direction with respect to the wellbore (a preferred fracture plane does not exist). On the other hand, if the stress anisotropy is 4,000 psi, it was shown that a single vertical fracture initiates for the perforations that are aligned within 5° from the preferred fracture plane.

A correlation between the stress anisotropy and the critical perforation orientation angle is developed. The critical perforation orientation angle is defined as the maximum allowable deviation angle from the preferred fracture plane within which a single vertical fracture initiates.

More than 25 simulation runs were made to investigate the effects of stress anisotropy on the critical perforation orientation angle. The simulation procedure is as follows:

- Use different stress anisotropy values (0 psi, 250 psi, 500psi, etc.).
- Use different orientation angles for each stress anisotropy value until a single vertical fracture initiates.
- Record the critical perforation orientation angle.

The above procedure is an iterative approach to determine the critical perforation orientation angle. The results of these simulation runs are plotted in Figure 13 in terms of the critical perforation orientation angle from the preferred fracture plane.

Effects of Perforation Phasing on Fracture Initiation

Perforation phasing significantly affects the hydraulic fracturing operation. Perforation phasing determines whether or not a high fracturing treating pressure is needed; moreover, it determines whether or not a complex geometry is induced in the near-wellbore region. Perforation phasing is defined as the angular spacing between each perforation in the gun system. A mesh that models a full wellbore with two perforations is used to investigate the effects of perforation phasing on fracture initiation. The first perforation is always aligned to 0° (parallel to the minimum horizontal principal stress) and the second perforation is rotated to different desired angles to simulate different phasing as shown in Figure 14 (180° phasing). For instance, the second perforation is oriented at an angle of 60° if a 60° phasing is desired and so on. Only two perforations were used because of the computational limitations and the complexity of the mesh generation.

Different perforation phasings were used to investigate the effects of perforation phasing on fracture initiation. The stress anisotropy, wellbore and perforation dimensions are listed in Table 3. The results obtained from the finite element program need to be visualized graphically. A typical output obtained from the finite element program has approximately 27,000 data points. Therefore, horizontal planes must be cut to ascertain the positions of fracture initiation. There is no clear communication between the perforations because fracture initiation is being modeled and not fracture propagation. However, results obtained from simulation runs provide some general understanding of where and how far into the perforation fractures might initiate.

90° Perforation Phasing

The full wellbore mesh with two perforations is used to model the 90° perforation phasing. The first perforation is oriented at 0° and the second perforation is oriented at 90° (preferred fracture plane). A relatively low fracturing pressure (10,500 psi) is calculated, since one of the perforations is perpendicular to the direction of the minimum horizontal in-situ stress. The results of this simulation run are illustrated in Figures 15 and 16. A single vertical fracture is initiated along the entire perforation tunnel for the perforation that was oriented at 90° as shown in Figure 16. Since the perforation is oriented towards the preferred fracture plane, the fracture initiates in the same plane in which it propagates. Therefore, a wide single vertical fracture will be created and a possible tortuous path and complex fracture geometry is eliminated. It is observed that a fracture did not initiate from the perforation that is oriented at 0° as illustrated in Figure 15. A relatively low fracturing pressure is needed to initiate a fracture for the perforation that is oriented in the preferred plane. On the other hand, a very high fracturing pressure must be applied to initiate a fracture along the entire perforation tunnel when the perforation is not aligned to the preferred fracture plane as

shown in Figures 15-16. When perforations are oriented in the preferred plane, the fracturing treating pressure is significantly reduced. The results of other perforation phasing simulation runs are listed in Table 4.

Oriented 180° Phasing

Perforation design using a 180° phasing in which both perforations are oriented in the preferred fracture plane direction is recommended. The tangential stress around the wellbore has the lowest value at the preferred fracture plane direction. Thus, a low fracturing pressure is needed to initiate a fracture. The fracture will initiate at the same plane through which it propagates and a classical bi-wing fracture is induced. The complex fracture geometry around the wellbore is theoretically eliminated. As a result, a large fracture width is obtained that provides an excellent communication between the wellbore and the induced fractures.

Conclusions

Effects of Perforation Orientation on Fracture Types

Perforation orientation as a function of the in-situ stress field significantly influenced the initiated fracture types. The following fracture types are induced (assuming stress anisotropy):

- A single vertical fracture initiates when the perforation orientation angle is greater than or equal to the critical perforation orientation angle.
- Multiple parallel fractures and S-shaped fractures initiate when the perforation orientation angle is less than the critical perforation orientation angle.
- An axial fracture or T-shaped fracture initiates when the perforation orientation angle is less than 10°, $\theta < 10$ (the exact value depending on the stress anisotropy value).

A correlation between stress anisotropy and the critical perforation orientation angle was developed. The correlation determines the critical perforation orientation angle that insures the initiation of a single vertical fracture for a given stress anisotropy value. The correlation also provides the maximum allowable deviation angle from the preferred fracture plane that insures the initiation of a single vertical fracture for a given stress anisotropy value.

Effects of Perforation Phasing on Fracture Initiation

Perforation phasing plays an important role in shaping the near wellbore fracture geometry. It determines whether or not a tortuous path that acts as an obstruction to the proppant placement is created. The following fracturing behaviors are observed:

- 180° non-oriented phasing, 120° phasing, 90° phasing, and 60° phasing have great potential to induce complex near-wellbore fracture geometry.
- 180° oriented phasing, in which the perforations are oriented toward the preferred fracture plane, induces a single vertical bi-wing fracture that helps in eliminating the complex near wellbore fracture geometry and creates accessible channels for the proppant to flow though.

Nomenclature

ΔP : Difference between wellbore pressure and formation pressure
r : Radius of any point in the formation with respect to the wellbore
r_w : Wellbore radius
θ : Orientation angle
σ_3 : Minimum principal stress
$\sigma_{H\min}$: Minimum horizontal in-situ stress
$\sigma_{H\max}$: Maximum horizontal in-situ stress
$\sigma_{\min}$: Minimum in-situ stress
σ_r : Radial stress
σ_T : Tensile strength
σ_θ : Tangential stress
$\tau_{r\theta}$: Shear stress in (r, θ) plane

References

1. Haimson, B. C. and Fairhurst, C., "Hydraulic Fracturing in Porous Permeable Material," Journal of Petroleum Technology, (1969), pp. 811-817.
2. Behrmann, L. A., Elbel, J.L., "Effect of Perforations on Fracture Initiation," SPE 20661, presented at the 65th Annual SPE Technical Conference and Exhibition, New Orleans, LA, (1990).
3. Morales, R.H., Brady, B.H., and Ingraffea, A.R., "Three Dimensional Analysis and Visualization of the Wellbore and the Fracturing Process in Inclined Wells," SPE Paper No. 25889, (Apr. 1993).
4. Yang, Z., Crosby, D.G., Akgun, F., Khurana, A.K., and Rahman, S.S., "Investigation of the Factors Influencing Hydraulic Fracture Initiation in Highly Stressed Formations", SPE Paper No. 38043, (Apr. 1997).
5. Weng, X., "Fracture initiation and Propagation from Deviated Wellbores," SPE Paper No. 26597, (Oct. 1993).
6. Akgun, F., Yang, Z., Crosby, D.G., and Rahman, S.S., "Factors Affecting Hydraulic Fracture Initiation in High In-Situ Stress Conditions: A Wellbore Stress Modeling Approach," SPE Paper No. 38631, (Oct. 1997).
7. Ebrahim, A., "Perforation Design for Fracture Stimulated Wells," Ph.D. Dissertation, Colorado School of Mines, (Dec. 1998).
8. Smith, I.M. and Griffiths, D.V. "Programing the finite

element method", 3rd edition, John Wiley & Sons, (1998)
9. Jaeger, J.C. and Cook, N.G.W., Fundamentals of Rock Mechanics, Halsted Press, New York City (1976).
10. Timoshenko, S. and Goodier, N. J., Theory of Elasticity, 2nd ed. McGrow Hill, New York (1951).
11. Valko, P and Economides M. J., "Hydraulic Fracture Mechanics," John Wiley & Sons, New York, (1995).
12. Taig, I.C., "Structural Analysis by the Matrix Displacement Method," English Electric Aviation Report No. 5017, (1961).
13. Abass, H. H., Hedayati, S., and Meadows, D. L., "Nonplanar Fracture Propagation From a Horizontal Wellbore: Experimental Study," SPE 24823, presented at the 67th Annual SPE Technical Conference and Exhibition, Washington D.C., (Oct. 1992).
14. Weijers, L., de Peter, C. J., Owens, K. A., Kogsboll, H. H., "Geometry of Hydraulic Fractures Induced From Horizontal Wellbores," SPE Production & Facilities, (May 1994), pp. 87-92.

Aknowledgment

The authors wish to thank the Production Enhancement Research FORuM (PERFORM) at the Colorado School of Mines for supporting this project. The sponsorship of member companies is recognized: AMOCO, ARCO, BJ Services, BP Exploration (Alaska), CARBO Ceramics, Marathon, Maxus, Mobil, and Union Pacific Resources.

Table 1
Parameters Used in Investigating the Effects of Perforation Orientation on Fracture Types.

Perforation Length	15 inches
Perforation Radius	0.25 inches
Maximum Horizontal Stress	10,500 psi
Minimum Horizontal Stress	6,500 psi
Vertical Stress	11,500 psi
Pore Pressure	5,250 psi
Poroelastic Constant	0.7
Casing Young's Modulus	30.0e6 psi
Casing Poisson's Ratio	0.3
Cement Young's Modulus	1.0e6 psi
Cement Poisson's Ratio	0.3
Sandstone Young's Modulus	3.0e6 psi
Sandstone Poisson's Ratio	0.3
Internal Friction Angle	30.0°
Shear Cohesion	5,600 psi
Sandstone Tensile Strength	500 psi

Table 2
Fracture Types as a Function of the Perforation Orientation Angle, Stress Anisotropy = 4,000 psi.

Perforation Orientation Angle °	Fracturing Pressure (psi)	Fracture Type
90	11,500	Single Vertical Fracture
85	11,500	Single Vertical Fracture
80	11,500	Multiple or S-Shaped Fracture
75	12,500	Multiple or S-Shaped Fracture
70	15,500	Multiple or S-Shaped Fracture
60	15,500	Multiple or S-Shaped Fracture
50	15,500	Multiple or S-Shaped Fracture
45	15,500	Multiple or S-Shaped Fracture
40	15,500	Multiple or S-Shaped Fracture
30	15,500	Multiple or S-Shaped Fracture
20	15,500	Multiple or S-Shaped Fracture
10	15,500	Multiple or S-Shaped Fracture
5	15,500	Axial or T-Shaped Fracture
0	17,500	Axial or T-Shaped Fracture

Table 3
Data Used in the Perforation Phasing Simulation Runs

Perforation Length	15 inches
Perforation Radius	0.25 inches
Maximum Horizontal Stress	10,500 psi
Minimum Horizontal Stress	6,500 psi
Vertical Stress	11,500 psi
Pore Pressure	5,250 psi
Poroelastic Constant, γ	0.7
Casing Young's Modulus	30.0e6 psi
Casing Poisson's Ratio	0.3
Cement Young's Modulus	1.0e6 psi
Cement Poisson's Ratio	0.3
Sandstone Young's Modulus	3.0e6 psi
Sandstone Poisson's Ratio	0.3
Internal Friction Angle	30.0°
Shear Cohesion	5,600 psi
Sandstone Tensile Strength	500 psi

Table 4
Effect of Perforation Phasing on Fracture Initiation

Perforation Phasing	Fracturing Pressure (psi)	Comments
180°, $\theta1 = 0°$, $\theta2 = 180°$	11,000	Fractures did not initiate in the perforation tunnel
180°, $\theta1 = 0°$, $\theta2 = 180°$	17,500	Fractures initiated in some areas in the perforation tunnel. T-shaped fracture
120°, $\theta1 = 0°$, $\theta2 = 120°$	17,500	Multiple fractures,
90°, $\theta1 = 0°$, $\theta2 = 90°$	10,500	Single vertical fracture at $\theta2$, no fracture initiation at $\theta1$. Single vertical fracture
60°, $\theta1 = 0°$, $\theta2 = 60°$	17,500	Same as 120° phasing
45°, $\theta1 = 0°$, $\theta2 = 45°$	17,500	Same as 120° phasing
30°, $\theta1 = 0°$, $\theta2 = 30°$	17,500	Multiple fractures

(A)

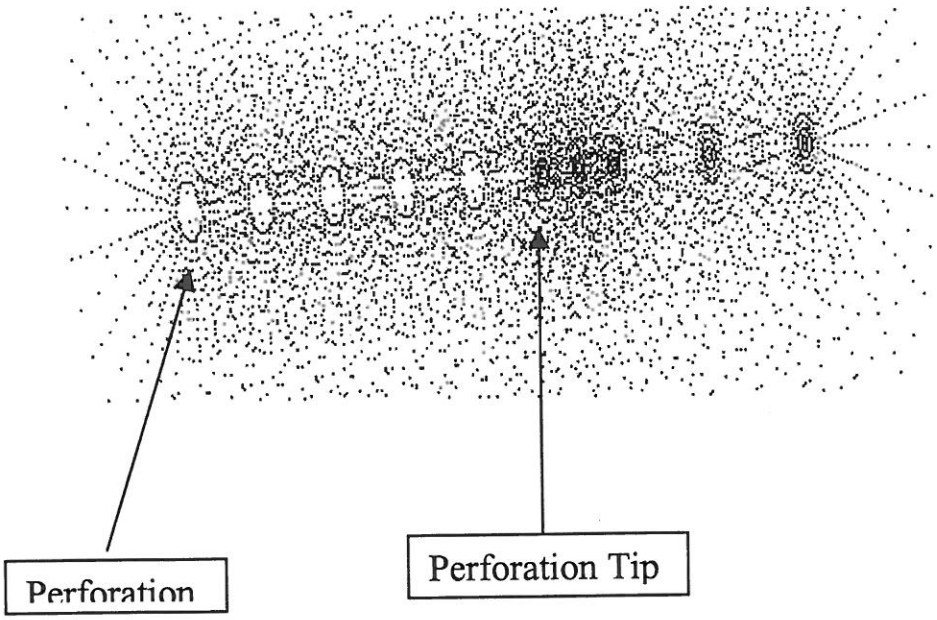

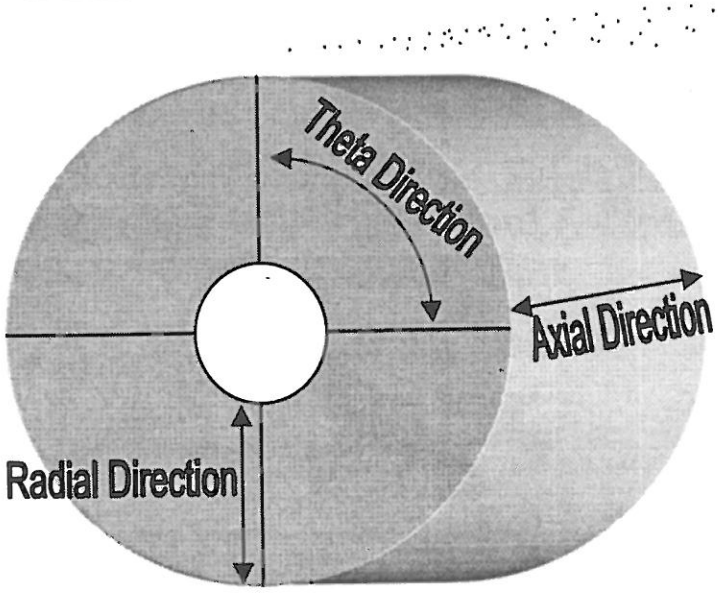

(B)

Figure 1: (A) Three-Dimensional Point Mesh of a Single Perforation, (B) Direction of Mesh Refinement

(A)

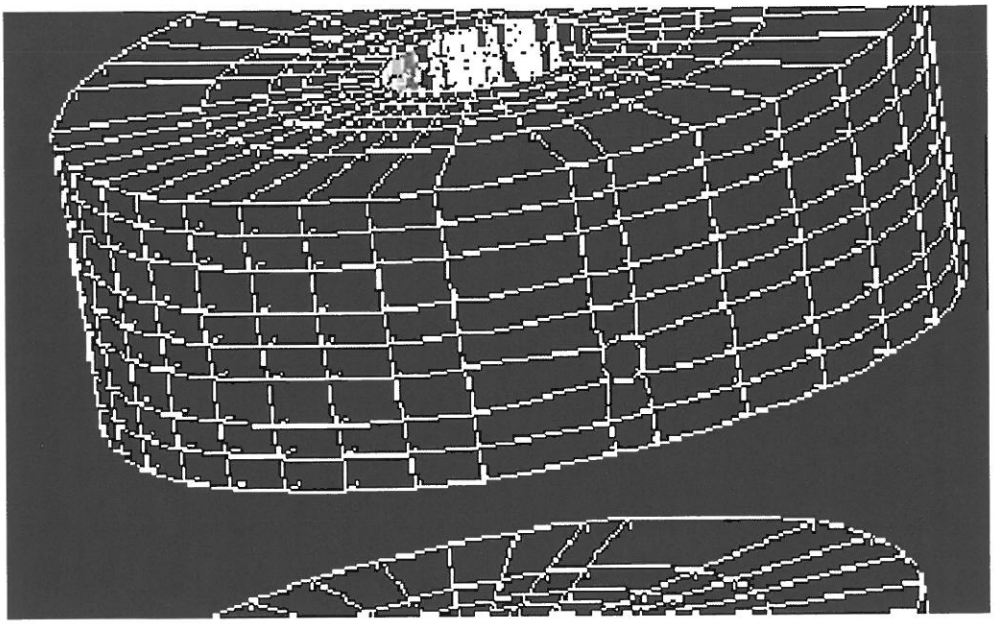

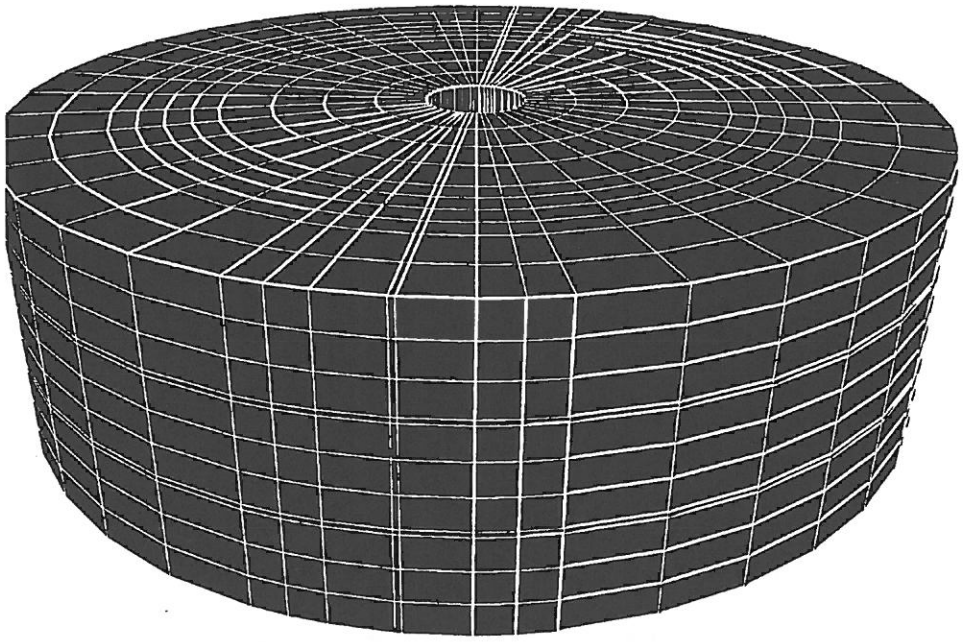

(B)

Figure 2: (A) Three-Dimensional Mesh of a Wellbore with Two Perforations, (B) Refined Three-Dimensional Mesh of a Wellbore with Two Perforations

(A) A Horizontal Plane Cut at the Top or Bottom of the Perforation Tunnel

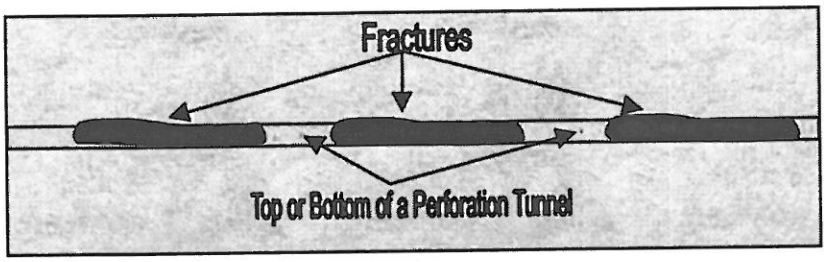

(B) A Horizontal Plane Cut at the Center of the Perforation Tunnel

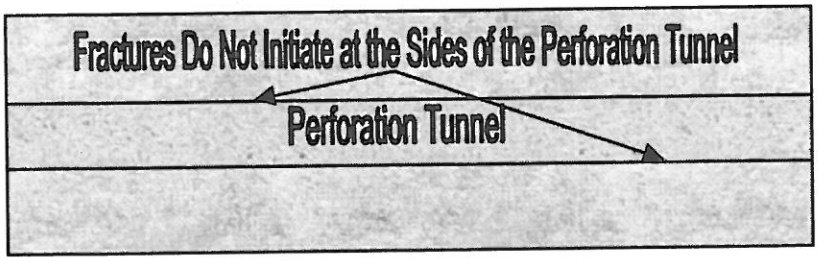

Figure 3: Identifying a Single Vertical Fracture

(A) Multiple Fracture

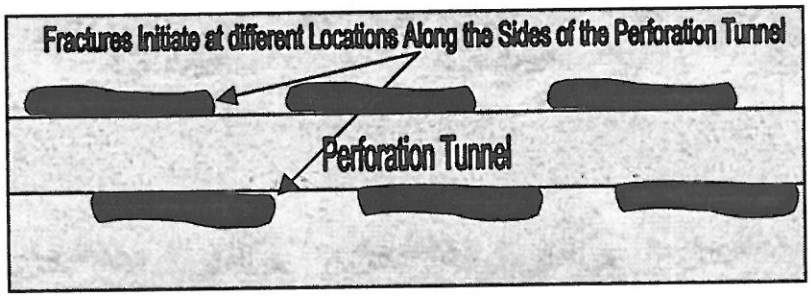

(B) Axial Fracture

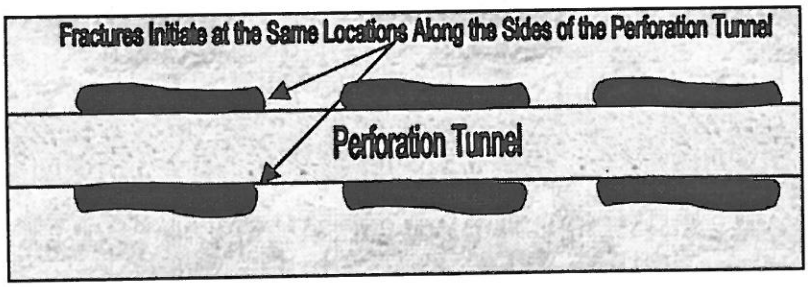

Figure 4: Identifying Multiple and Axial Fractures

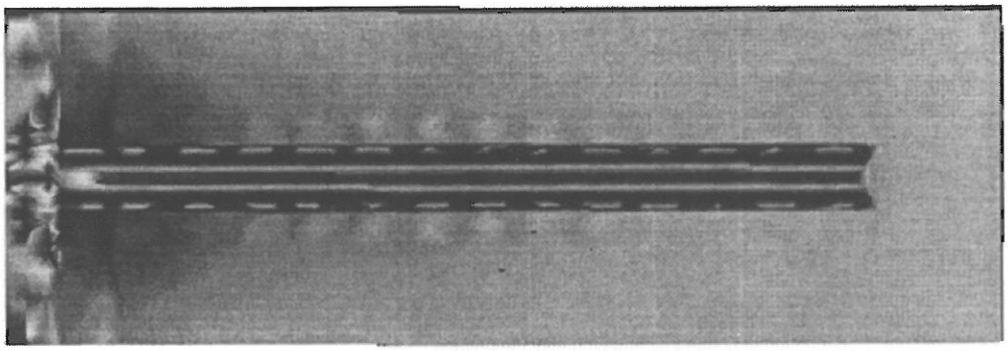

Figure 5: Contouring the Mohr-Coulomb (F). A Horizontal Cut at the Bottom of the Perforation that is Refined in the Axial Direction, $\theta = 90°$

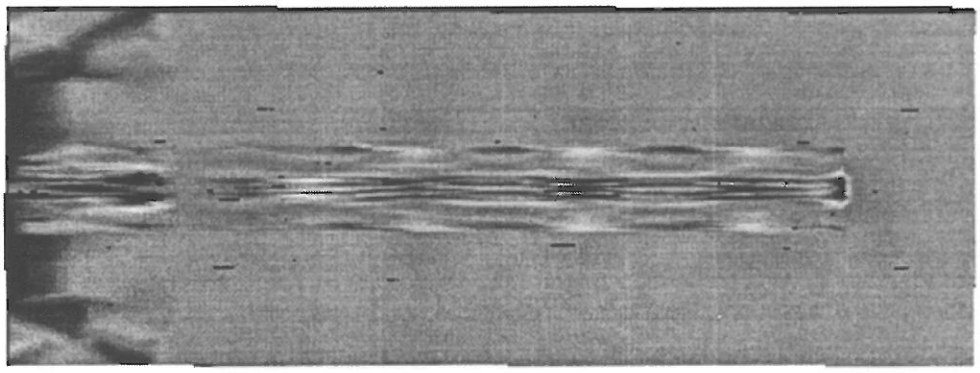

Figure 6: Contouring the Mohr-Coulomb (F). A Horizontal Cut at the Bottom of the Perforation, $\theta = 90$

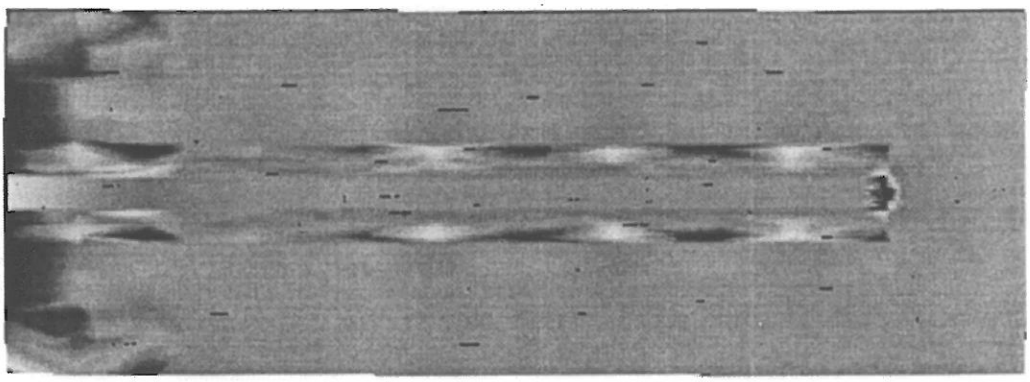

Figure 7: Contouring the Mohr-Coulomb (F). A Horizontal Cut at the Center of the Perforation, θ = 90°

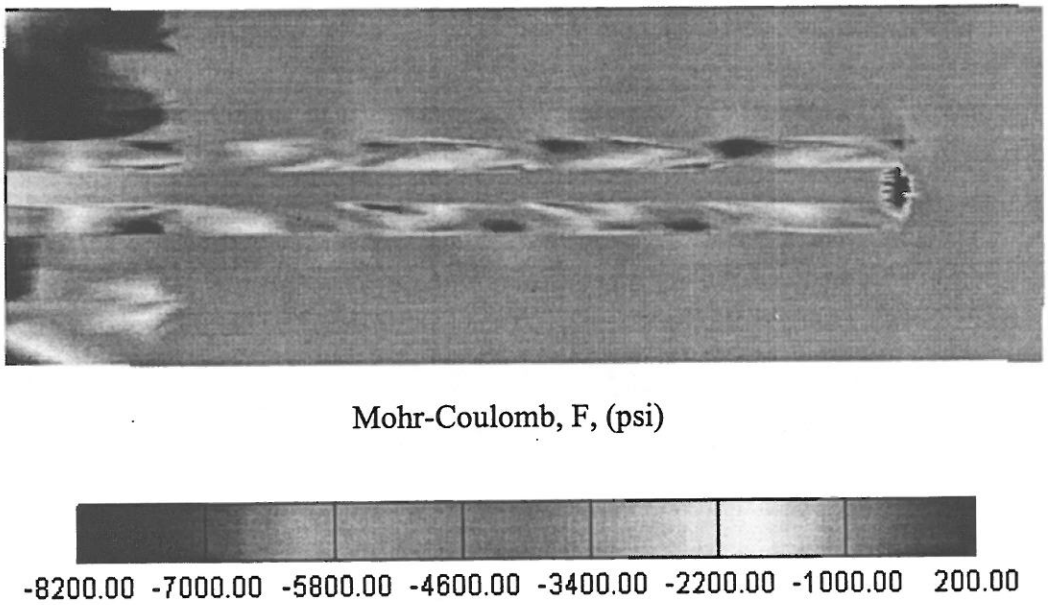

Figure 8: Contouring the Mohr-Coulomb (F). A Horizontal Cut at the Center of the Perforation that is Refined in the Axial Direction, θ = 60°

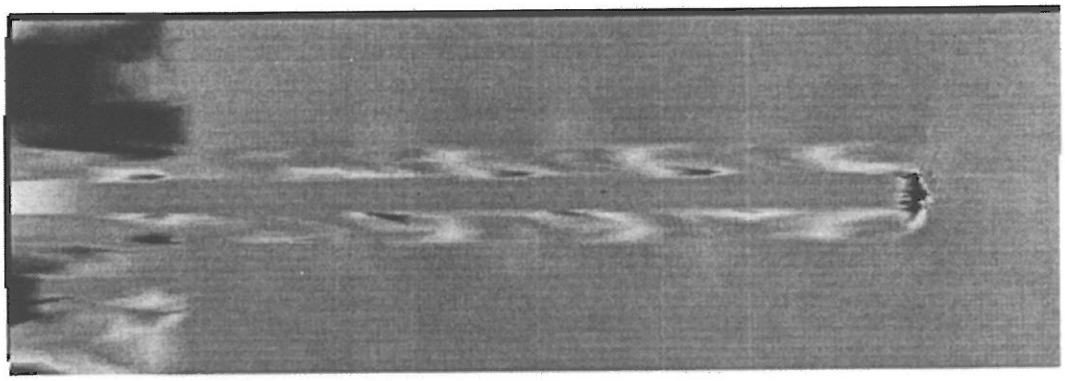

Mohr-Coulomb, F, (psi)

-8200.00 -7000.00 -5800.00 -4600.00 -3400.00 -2200.00 -1000.00 200.00

Figure 9: Contouring the Mohr-Coulomb (F). A Horizontal Plane Cut at the Center of the Perforation, $\theta = 30°$

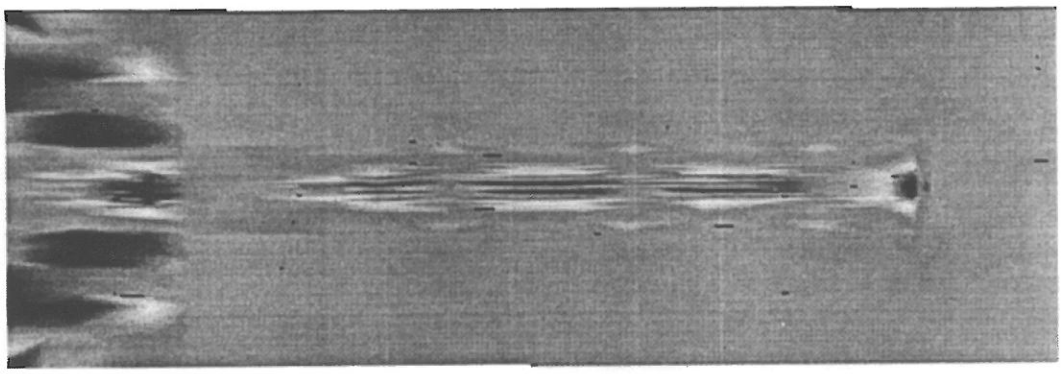

Mohr-Coulomb, F, (psi)

-8200.00 -7000.00 -5800.00 -4600.00 -3400.00 -2200.00 -1000.00 200.00

Figure 10: Contouring the Mohr-Coulomb (F). A Horizontal Cut at the Bottom of the Perforation, $\theta = 0°$

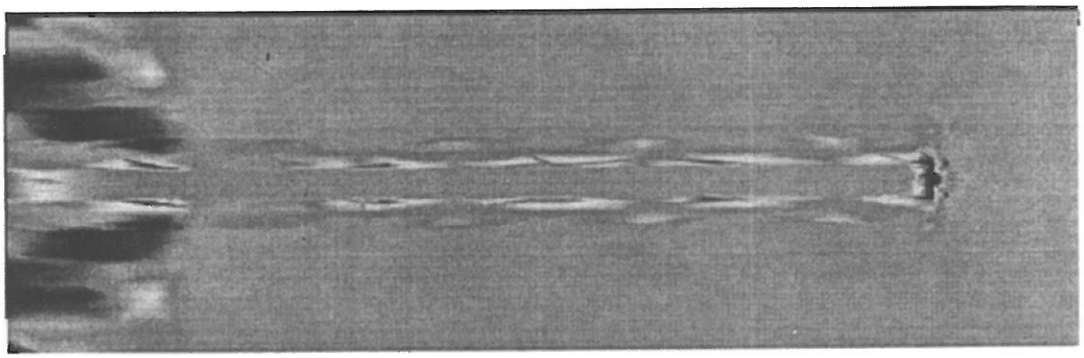

Figure 11: Contouring the Mohr-Coulomb (F). A Horizontal Plane Cut at the Center of the Perforation, θ = 0°

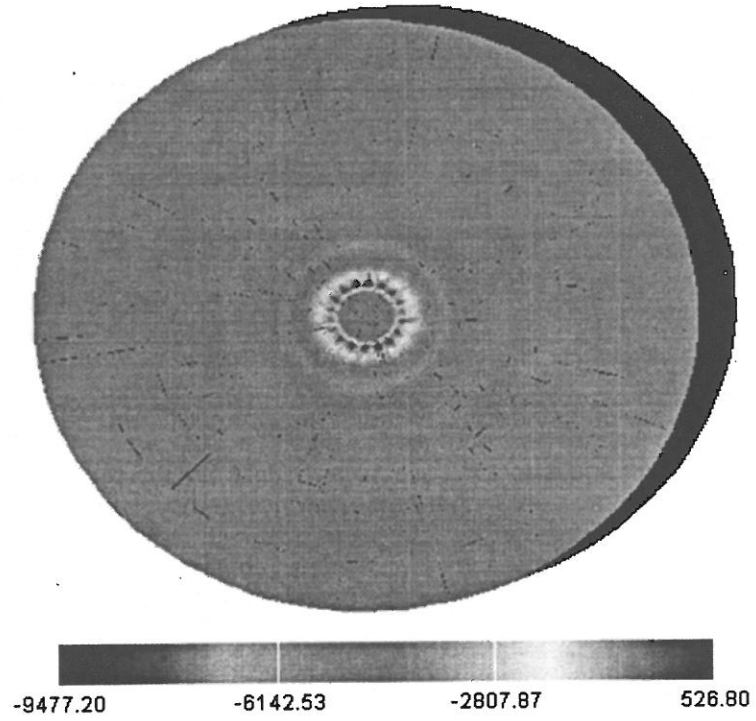

Figure 12: Contouring the Mohr-Coulomb (F). A Vertical Plane Cut at 9. Inches Along the Perforation Tunnel, θ = 0°

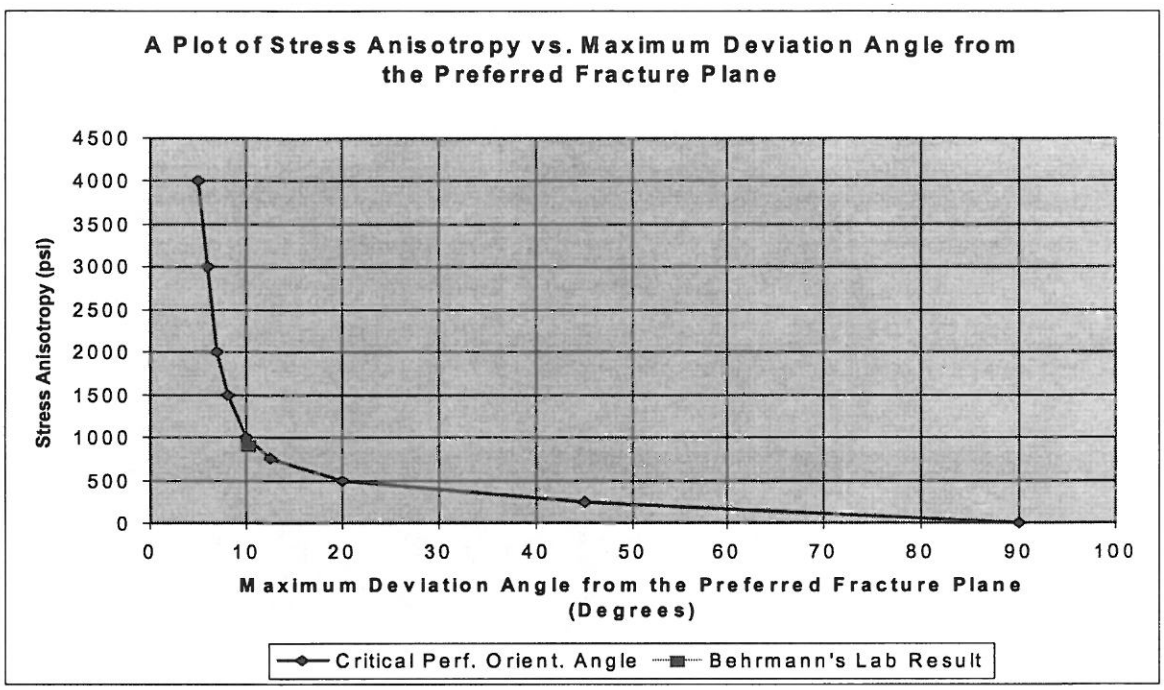

Figure 13: A Correlation Between Stress Anisotropy and the Maximum Allowable Deviation Angle from the Preferred Plane, Using the Tensile Failure Criteria

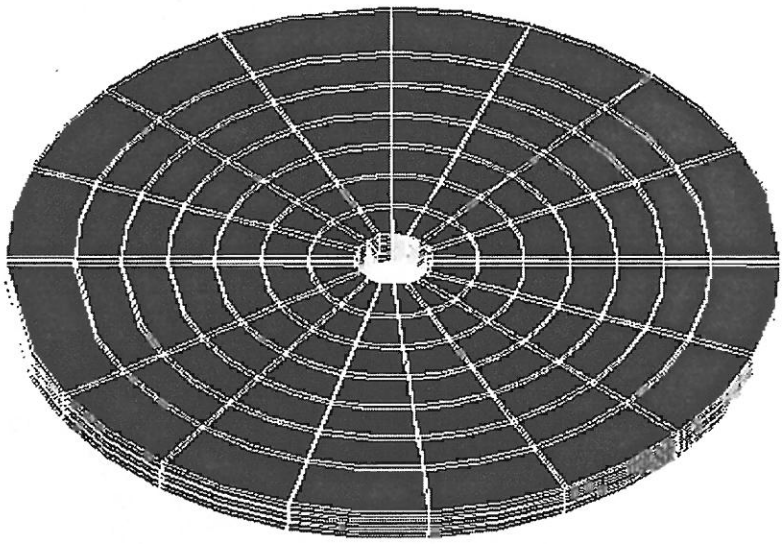

Figure 14: Three-Dimensional Mesh Used to Model a 180° Phasing

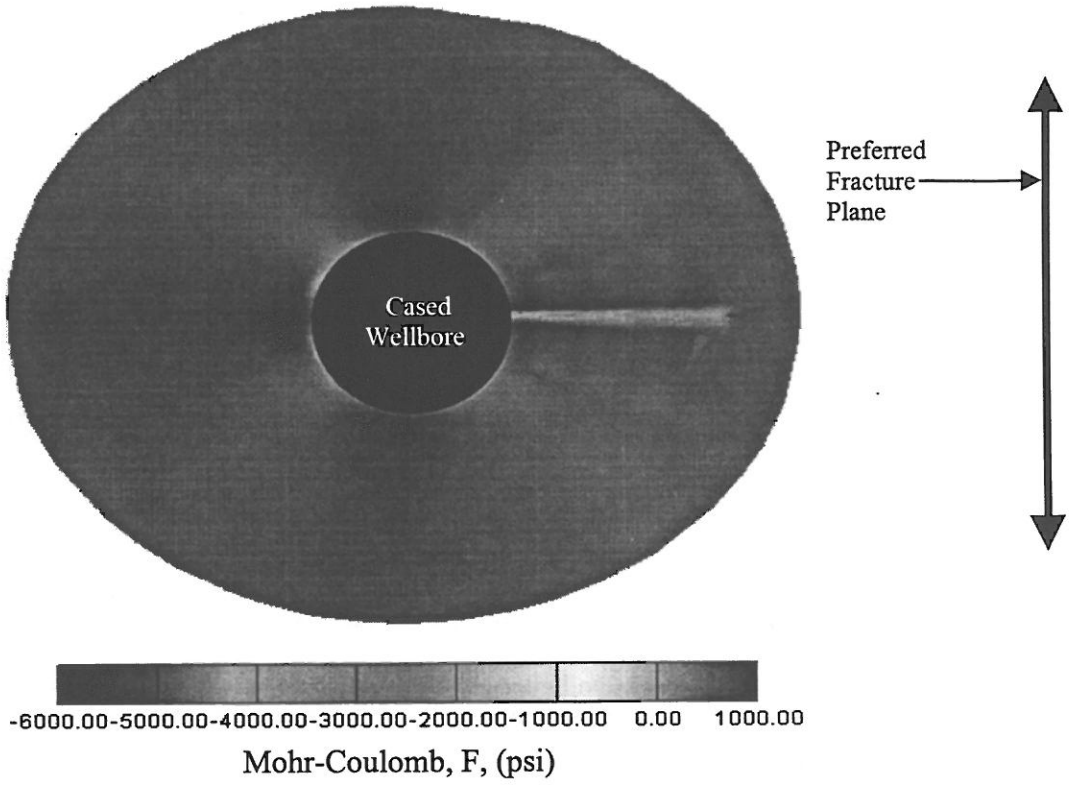

Figure 15: Contouring the Mohr-Coulomb (F). A Horizontal Plane Cut at the Bottom of the First Perforation that is Oriented at 0°, Fracture Pressure = 10,500 psi

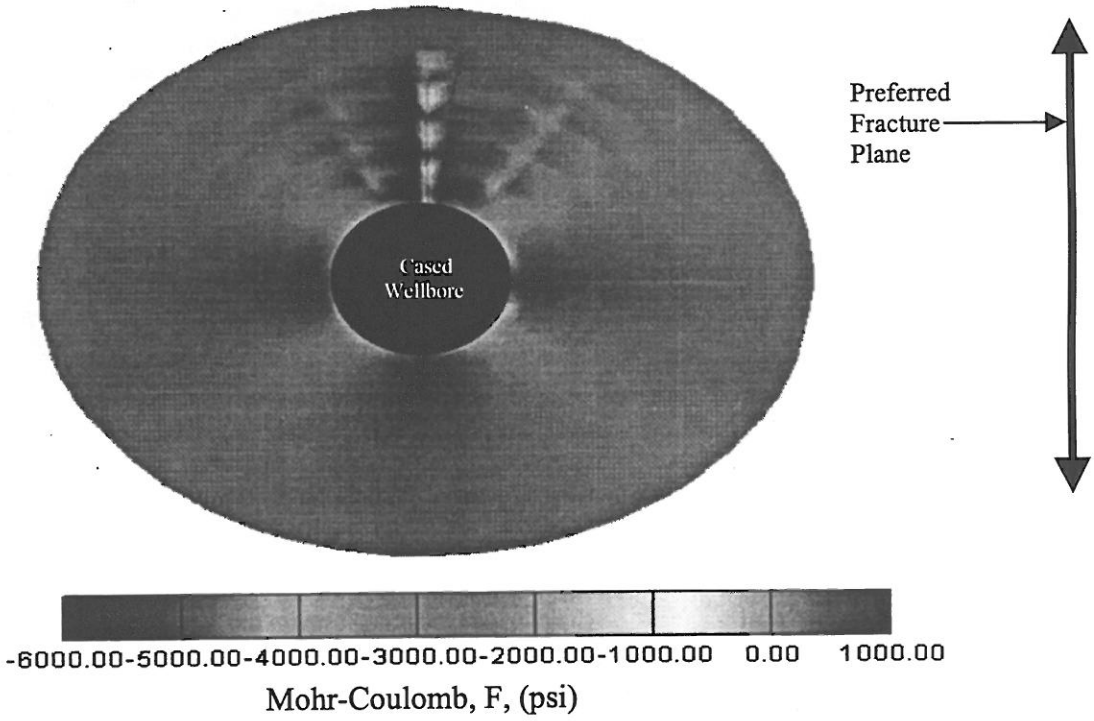

Figure 16: Contouring the Mohr-Coulomb (F). A Horizontal Plane Cut at the Bottom of the First Perforation that is Oriented at 90°, Fracture Pressure = 10,500 psi